QUANTUM SEARCH IN SUPERPOSED QUANTUM LATTICE GAS AUTOMATA AND LATTICE BOLTZMANN SYSTEMS

A PREPRINT

© Călin A. Georgescu
Delft University of Technology
Mekelweg 4, 2628CD, Delft
c.a.georgescu@tudelft.nl

• Matthias Möller Delft University of Technology Mekelweg 4, 2628CD, Delft m.moller@tudelft.nl

October 17, 2025

ABSTRACT

As the scope of Computational Fluid Dynamics (CFD) grows to encompass ever larger problem scales, so does the interest in whether quantum computing can provide an advantage. In recent years, Quantum Lattice Gas Automata (QLGA) and Quantum Lattice Boltzmann Methods (QLBM) have emerged as promising candidates for quantum-native implementations of CFD solvers. Though the progress in developing QLGA and QLBM algorithms has been significant, it has largely focused on the development of models rather than applications. As a result, the zoo of QLGA and QLBM algorithms has grown to target several equations and to support many extensions, but the practical use of these models is largely limited to quantum state tomography and observable measurement. This limitation is crucial in practice, because unless very specific criteria are met, such measurements may cancel out any potential quantum advantage. In this paper, we propose an application based on discrete optimization and quantum search, which circumvents flow field measurement altogether. We propose methods for simulating many different lattice configurations simultaneously and describe how the usage of amplitude estimation and quantum search can provide an asymptotic quantum advantage. Throughout the paper, we provide detailed complexity analyses of gate-level implementations of our circuits and consider the benefits and costs of several encodings.

Keywords Quantum Computing · Lattice Gas Automata · Lattice Boltzmann Method · Computational Fluid Dynamics · Quantum Algorithm

1 Introduction

Scientific computing has become and indispensable pillar of the modern scientific and engineering landscapes, spanning fields that affect nearly all levels of society. Of the computational sciences, Computational Fluid Dynamics (CFD) stands out as a particularly versatile tool. In the aerospace industry, for instance, advances in CFD are crucial for improving the design of aircraft components and for lowering the high cost incurred by running experiments [44]. To realize simulations of the scale and precision required for such applications, it is common for solvers to utilize thousands of compute nodes to solve systems with hundreds of millions or billions of unknowns [44]. One of the critical challenges that solvers must overcome to accommodate ever larger industrial demands comes from hardware limitations. In contrast to the sustained and rapid advancement of hardware capabilities over the last decades, recent hardware progression has been decelerating. Faced with the long predicted slowdown of Moore's Law [55], scientists and engineers have turned their attention to alternative paradigms, including quantum computing [25].

The first exploratory studies of quantum computing for CFD date back to the latter half of the 1990s [45, 69] and focus on the development of the first Quantum Lattice Gas Automata (QLGA) systems. Though several other branches of Quantum CFD methods have since developed [21, 41, 12, 16], QLGA and the related Quantum Lattice Boltzmann Method (QLBM) have been receiving increasing amounts of interest in recent years. The QLGA and QLBM research landscape spans many applications, including transport methods [59, 53], the advection-diffusion equation [9, 64, 65],

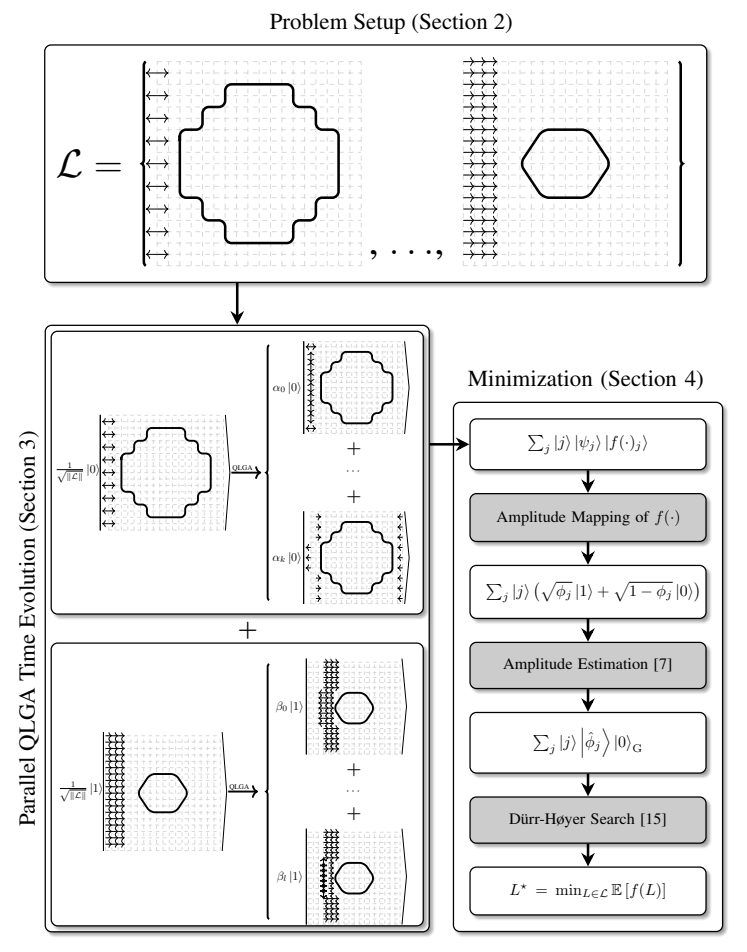


Figure 1: Overview of the quantum search algorithm with over superposed QLGA states.

the Navier-Stokes equations [9, 56, 36, 62], as well as linearization techniques [35, 51] and algorithmic extensions [73, 74, 19, 18, 22, 42]. This recent body of work has largely focused on model development, and has shown that QLGA and QLBM algorithms are promising candidates for the future development of quantum CFD solvers.

However, one key challenge that remains unaddressed in this research is the application of these models. In much of the literature, models are validated against classical counterparts by comparing the flow field extracted from the quantum state inferred by the model. Though crucial for validation, this method is infeasible for practical uses of the model, as it requires quantum state tomography (QST) to sufficiently approximate the quantities encoded in the quantum state. Clearly, any computational advantage attained by the model up to measurement is lost in this scenario. Previous work by Schalkers and Möller [54] and Georgescu et al. [22] has formulated observables for the extraction of Quantities of Interest (QoIs) out of the quantum state for several physical properties, but the efficiency of these methods is highly dependent on the simulation and only preserves the advantage in limited scenarios.

In this paper, we propose a novel application of QLGA and QLBM models that is practically relevant and entirely circumvents the measurement of the flow field. In particular, we focus on *discrete optimization* scenarios, in which we are interested in problems where we aim to find the best candidate solution out of a given input set. We introduce a novel *parallel time-evolution* extension to QLGA and QLBM algorithms that enables multiple systems to be simulated simultaneously. We provide quantum circuits that efficiently accumulate QoIs in quantum state using light-weight implementations. To solve the minimization problem, we use established quantum algorithms, including amplitude estimation [7] and the Dürr-Høyer minimum finding algorithm [15] to obtain a quadratic asymptotic computational advantage compared to classical counterparts. Throughout the paper, we give gate-level descriptions of the circuits we introduce and analyze their complexity under practical assumptions. Up to the measurement required by the minimum-finding routine, our algorithm is entirely coherent. To the best of our knowledge, this marks the first connection between fields of Quantum CFD and Optimization fields.

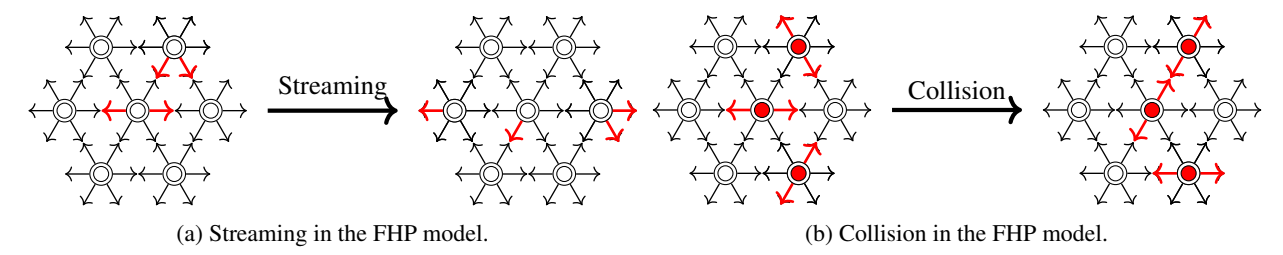


Figure 2: Example of lattice states, streaming, and collision in the FHP model [20].

Figure 1 provides an end-to-end overview of our algorithm, which consists of three distinct stages. The first stage samples several lattice configurations and formulates the optimization as described in Section 2. The second stage performs the parallel time-evolution of all sampled systems with either the QLGA or QLBM algorithms, as detailed in Section 3. Following the time-evolution of the system, the third and final stage transforms the quantum state such that amplitude estimation and minimum finding routines can solve the minimization problem with a quadratic asymptotic quantum advantage, as outlined in Section 4. Finally, Section 5 concludes the paper.

2 Preliminaries

This section provides the necessary background and definitions that our algorithm is built on top of. For the remainder of the paper, we frame the description of our methods for linear encoding of the QLGA algorithm, as it provides the both the most challenges and the most opportunities. We address typical QLBM encodings and complexities in Section 3.4, and note fundamental differences wherever they arise. We first describe the linear QLGA encoding we use throughout the rest of the paper, before formalizing the problem statement. Finally, we provide a succinct overview of the unstructured search, amplitude estimation, and minimum finding quantum algorithms.

2.1 Quantum Lattice Gas Automata and Quantum Lattice Boltzmann Methods

The origins of Cellular Automata (CA) can be traced back to the seminal works on foundational models of computation by John von Neumann and Arthur Burks around the middle of the 20th century [60]. In a general sense, CA models consist of structured arrangements of discrete cells, which are assigned one of a finite number of discrete states, and evolve according to a set of rules that are applied simultaneously to all cells [68]. The work of Hardy et al. [29] in 1973 is the first application of CA in the domain of computational physics and marks the emergence of the Lattice Gas Cellular Automata (LGA) subfamily of CA. This first LGA model introduced a 2-dimensional grid structure of cells arranged in a square structure with links to their nearest neighbors in both directions of either dimension. Particle behavior is governed by particle transport (streaming) and particle-particle interactions (collisions) that change the course of particles upon intersection. The more complex hexagonal grid LGA model of Frisch et al. [20] later superseded its predecessor as its larger symmetry group can be shown to lead to the incompressible Navier-Stokes equations in the hydrodynamic limit [68]. These models are known in the literature as the HPP [29] and FHP [20] models, respectively.

One key distinction between CA and LGA is the physical interpretation assigned to states of the grid. Generally, an LGA gridpoint consists of several distinct *velocity channels*, which act as means of propagating information between gridpoints. The LGA grid is populated by discrete particles, which have pre-determined properties and are indistinguishable from one another. The state of an LGA gridpoint is determined by whether each of its velocity channels is occupied by a particle. Since particles are indistinguishable, this state can be modelled as a bitstring whose length is equal to the number of velocity channels. The rules that govern the behavior of LGA – streaming and collision – are visually depicted in Figure 2 for the FHP discretization. Figure 2a shows how particles (highlighted in red) stream along velocity channels, while Figure 2b portrays how collision stochastically redistributes particle occupancies (at the highlighted gridpoints) such that mass and momentum are conserved. This straightforward physical discretization leads naturally to the computation of physical properties of the system, such as mass and momentum-density [68]. A general description of QLGA for arbitrary velocity discretizations is given in Georgescu et al. [22].

Around a decade after the development of the FHP model, interest in the quantum realization of LGA began to surge. The first Quantum Lattice Gas Automata models were developed by Meyer [45, 46], Boghosian [4, 5], and Yepez [69, 70, 71, 72] and established the feasibility and limitations of implementing the stream-collide semantics of LGA on quantum computers. However, shortly after the turn of the century, as classical CFD methods greatly benefitted from the unprecedented growth fueled by the rapid improvement of computer hardware, the largely theoretical QLGA research

experienced a decline in interest. Following nearly two decades of stagnation, the resurgence in QLGA research occurred in the late 2010s as researchers again turned their attention to potential CFD Applications of quantum computing. Love [43] introduced quantum circuits for the collision and propagation steps for several 1- and 2-dimensional QLGA models. Fonio et al. [19], Kocherla et al. [39], and Georgescu et al. [22] introduce extensions to the initialization, streaming, collision, and measurement steps of the QLGA loop. Fonio et al. [19] and Zamora et al. [73] utilize a compressed encoding, which more efficiently represents the state of a lattice at the cost of performing restarts following every time step. Zamora et al. [74] and Fonio et al. [18] introduce quantum algorithms based on variations of the Integer LGA – a model which replaces the boolean interpretation of particles with numerical values.

In this work, we focus our analysis on the *linear encoding* discussed in [43, 39, 22], which maps bits and qubits bijectively. Though this encoding offers no direct memory advantage, it allows for the simulation of arbitrarily many coherent time steps and simultaneous representation of exponentially many lattice states [53, 19, 62]. The representational power of this encoding is important, as QoIs are generally computed in terms of *ensemble averages* over many stochastic outcomes [68]. As we cover in the following sections, the linear encoding provides further computational advantages that are lost when information is compressed into fewer qubits.

Relation to Random and Quantum Walks. The boolean-particle LGA algorithm can be interpreted as a random walk over a weighted directed graph G=(V,E), where the vertex set V is the set of all attainable lattice configurations, and the edge set E is determined by the collision semantics of the system. Applying the typical collision operators, which preserve macroscopic quantities such as mass and momentum, one can define the stochastic physical semantics in terms of transition probabilities of a Markov chain traversal of G. For a number of gridpoints N_g and a discretization of q velocity channels, the size of the state space is $\mathcal{O}(2^{qN_g})$. Analogously, the QLGA algorithm can be interpreted as a discrete-time quantum walk, where branching occurs every LGA step by means of the collision step, while the streaming step maps each state to a neighboring vertex. For simulating a large number of time steps – and therefore a sizeable proportion of the Markov state space – the bijective linear encoding becomes necessary to simultaneously accommodate all outcomes. For thorough analyses of quantum walks and the broader field of quantum cellular automata, we refer the reader to references [61] and [17], respectively.

2.1.1 Quantum Lattice Boltzmann Methods

The Lattice Boltzmann Method [57, 40] has historically succeeded LGA as a computational approach for fluid flow problems. The core addition of the LBM is the introduction of a global distribution function that replaces the boolean particle discretization of its predecessor. This leads to significant noise reduction, as the LBM inherently tracks the averaged behavior of fluid at the mesoscopic scale, rather than the individual trajectory of each particle as in LGA. To accommodate this smoother discretization, the collision step of the LBM departs from the granular particle redistributions of the LGA models and is instead defined as a change in the local distribution associated with each gridpoint. The Bhatnagar-Gross-Krook (BGK) [3] collision operator is one of the simplest and most common implementation of the collision operator, which can still recover the bulk Navier-Stokes properties, and can be seen as a relaxation of the local distribution towards equilibrium.

Interest in the quantum analog of the LBM began to surge in the early 2020s with works such as those of Budinski [9, 10] and Steijl [56]. Though QLBM research has progressed significantly, two of the main open challenges are the modelling of nonlinearity and dissipation. The BGK [3] collision operator and more sophisticated counterparts that solve the Navier-Stokes equations all require the computation of quadratic terms used in irreversible updates of the distribution function. Since this operation is not directly implementable in the common quantum encodings used in the literature, much of the QLBM research has focused on developing suitable approximations of the collision process. This includes the usage of the Linear Combination of Unitaries [11] by Budinski [10], approximating the collision process by Carleman Linearization [35, 50], applying a classical correction step to the quantum state [62], and learning a linear approximation of the collision [42, 34]. To utilize the methods described in this paper, we only require that the QLBM solver is coherent, and assume that it uses an amplitude-based encoding, *i.e.*, that the value of the distribution function is encoded in the amplitude of each basis state. Two recently proposed approaches that fall into this category include the heat-transfer QLBM solver of Jawetz et al. [37] and the advection-diffusion solver of Nagel and Löwe [48].

Nomenclature and Complexity Analaysis. Throughout this paper, we provide circuit-level complexity analyses of the proposed algorithms. To do this, we assume an all-to-all connectivity of logical qubits, and we measure complexity in terms of 1- and 2- qubit gate decompositions. If no efficient decomposition is known for a particular gate, we assume its decomposition is exponentially expensive in the number of qubits it spans. We use the notations $N_{q,(\cdot)}$ and $N_{t,(\cdot)}$ to denote the number of qubits and time steps associated with a particular component of the algorithm, respectively. Finally we denote the application of a gate U with p controls as C^pU .

2.2 Problem Statement

We describe our algorithms as solvers for an optimization problem that is formulated as follows. Let \mathcal{L} be the set of lattice configurations that share the same spatial, temporal, and velocity discretizations, but that differ in either (i) initial conditions or (ii) boundary conditions. For each lattice $L \in \mathcal{L}$, let $f(L, \Omega, t) \in \mathbb{R}$ be the value of some scalar quantity of interest (QoI) computed over the physical region of space Ω of L at time L. We use the shorthand notation

$$f(L,\Omega) = \sum_{t \in \mathcal{N}_{t,acc}} f(L,\Omega,t)$$
 (1)

to denote the cumulative value of the quantity of interest over a specific set of discrete time steps $\mathcal{N}_{t,acc}$. Finally, let $LGA(L, N_t)$ be the probability distribution that arises after the time-evolution of lattice configuration of the lattice L for N_t time steps by the LGA algorithm. In this work, we are concerned with finding the lattice configuration

$$L^{\star} = \min_{L \in \mathcal{L}} \mathbb{E}_{x \sim \text{LGA}(L, N_t)} \left[f(x, \Omega) \right], \tag{2}$$

for a pre-defined lattice configuration L, QoI f and region Ω . That is, the lattice for which the QoI is minimal in the expectation over the ensemble average that emerges from nondeterminstic collision¹. Practically, the QoI encoded in the function f could be the drag coefficient of an airfoil, or the average pressure over a region of interest. The set \mathcal{L} could consist of several airfoil designs subject to the same initial conditions, or distinct set of initial conditions applied to the same geometry.

The QLBM counterpart of the problem statement is similar, but contains two key differences. First, the ensemble averaging that QLGA relies on is no longer required in the QLBM setting. Second, we restrict ourselves to the computation of the QoI for a single time step. This is not a theoretical limitation, but rather a practical consideration that stems from the amplitude-based encoding that is typical of QLBM methods. Estimating the mean value of an amplitude over multiple time steps is possible, but would utilize circuits whose complexity would dominate the typical QLBM time step.

2.3 Amplitude Amplification, Estimation, and Quantum Search

This section briefly reviews the key concepts behind the Quantum Amplitude Amplification (QAA), Quantum Amplitude Estimation (QAE), and Quantum Search algorithms. We begin with a short description of Grover's celebrated algorithm for unstructured database search.

2.3.1 Unstructured Database Search and Grover's Algorithm

The unstructured database search problem consists of (efficiently) searching a structureless table T of N entries where $T[j] \in \{0,1\} \ \forall \ j \in \{0,...,N-1\}$. The goal is to output an index j such that T[j] = 1, if one exists. Throughout this work, we are concerned with the case where t such entries exist, for an unknown number $t \geq 1$. The complexity of an algorithm for this problem is typically measured in the number of times the algorithm *queries* the table T, *i.e.*, the number of times an item of T is accessed. Classically, algorithms that solve the unstructured database search problem can be reduced to sampling a hypergeometric distribution without replacement, yielding an expected number of queries that is $\mathcal{O}(N/t)$. One of the most celebrated results in quantum computing stems from Grover's algorithm [27, 28] that has been shown to solve the unstructured database search problem using quadratically fewer queries.

To understand Grover's algorithm, we can partition the table T into two sets

$$\begin{cases}
A_0 = \{j \mid T[j] = 0\}, \\
A_1 = \{j \mid T[j] = 1\}
\end{cases}$$
(3)

with A_1 the set of solutions and A_0 the set of non-solutions. Grover's algorithm begins by initializing a register in the uniform superposition

$$|u\rangle = \sum_{j=0}^{N-1} \frac{1}{\sqrt{N}} |j\rangle = \sum_{j \in A_1} k_0 |j\rangle + \sum_{j \in A_0} l_0 |j\rangle = \sqrt{\frac{\|A_1\|}{N}} |A_1\rangle + \sqrt{\frac{\|A_0\|}{N}} |A_0\rangle, \tag{4}$$

¹Maximization is also trivially realizable by adjusting the threshold and Grover oracle in the Dürr-Høyer step.

with $k_0=l_0=1/\sqrt{N}$. Grover's algorithm can be interpreted as a series of two-dimensional rotations in the space spanned by $|A_1\rangle$ and $|A_0\rangle$ (often referred to as the "good" and "bad" states), where each rotation is composed of reflections about the $|A_1\rangle$ and $|u\rangle$ states, respectively. This operation is known as the Grover iterator

$$\mathcal{G} = \underbrace{\left(\mathbf{H}^{\otimes n} \mathbf{S}_0 \mathbf{H}^{\otimes n}\right)}_{=2|u\rangle\langle u|-\mathbb{I}} S_T, \tag{5}$$

where S_T is a *phase query gate* that acts as $S_T |x\rangle = -1^{T[x]} |x\rangle$, and $S_0 = 2 |0\rangle^{\otimes n} \langle 0|^{\otimes n} - \mathbb{I}$ is the reflection about the $|0\rangle^{\otimes n}$ state. After j executions of the Grover iteration, the coefficients can be geometrically interpreted as

$$\begin{cases} k_j = \frac{1}{\sqrt{t}} \sin((2j+1)\theta), \\ l_j = \frac{1}{\sqrt{N-t}} \cos((2j+1)\theta), \end{cases}$$
 (6)

where the angle θ satisfies $\sin^2 \theta = t/N$. Intuitively, the goal is to select an integer number of iterations such that the rotations move the state close to the good state $|A_1\rangle$, or, equivalently, such that l_j is close to 0. For an in-depth analysis of the case where the number of solutions is unknown, we refer the reader to the works of Boyer et al. [6] and Brassard et al. [7], where it is shown that the number of queries required for this case is $\mathcal{O}(\sqrt{N/t})$.

2.3.2 Quantum Amplitude Amplification and Estimation

Quantum Amplitude Amplification (QAA) [7] is a generalization of Grover's original unstructured database search algorithm [27, 28]. Applied to the same setting described in Section 2.3.1, QAA is tasked with increasing the probability of measuring the "good" state $|A_1\rangle$ by means of the Grover iterator. In this interpretation, the QAA algorithm can be understood as increasing the amplitude of $|A_1\rangle$ by roughly a constant at each iteration, leading to a quadratic improvement in the probability of measuring this state at the end of the execution [7].

Quantum Amplitude Estimation (QAE) is an extension of QAA, in which we are interested in estimating the probability of measuring the good state $a = \langle A_1 | A_1 \rangle$ as given in Equation (4), or, equivalently, estimating α in a quantum state state of the form $\sqrt{\alpha} | 1 \rangle + \sqrt{1-\alpha} | 0 \rangle$. The first formulation of QAE was proposed by Brassard et al. [7], and uses several applications of the iterator in Equation (5) controlled on the state of an ancillary register mapped to the Fourier basis. QAE leverages the sinusoidal form of the amplitudes in Equation (6) to estimate the angle $\theta \in [0, \pi/2]$ and therefore obtains an estimate $\hat{\alpha} = \sin^2(\pi y/N)$ for the state y measured in the ancillary register [7]. This method – applying multiple controlled Grover iterators followed by the inverse QFT – closely resembles Quantum Phase Estimation (QPE) and has become known as the *canonical* QAE in the literature. The canonical QAE requires a query complexity of $\mathcal{O}(\epsilon^{-1})$ for an additive error ϵ , which is in alignment with the theoretical bounds derived by Nayak and Wu [49], and a quadratic improvement over the classical $\mathcal{O}(\epsilon^{-2})$. The Grover operator used in this algorithm is given by

$$Q = AS_0 A^{\dagger} S_T, \tag{7}$$

with S_0 and S_T defined as in the Equation (5), while \mathcal{A} denotes the coherent quantum algorithm that acts as

$$\mathcal{A} |0\rangle^{\otimes n} |0\rangle = \sqrt{\alpha} |A_1\rangle |1\rangle + \sqrt{1-\alpha} |A_0\rangle |0\rangle. \tag{8}$$

In recent years, several approaches have emerged, that seek to reduce the cost of QAE by reducing its reliance on the QPE building blocks, while retaining its query advantage. Suzuki et al. [58] introduced a variant of QAE, which samples several applications of the Grover iterator and approximates α classically by means of maximum likelihood estimation. Wie [66] introduces an alternative QAE algorithm that relies on applications of controlled Grover iterators with increasingly many controls, without requiring the use of the QFT, and instead relying on the Hadamard test. Aaronson and Rall [1] provide an analysis of another QAE variant that resembles binary search over the number of applications of Grover iterators. Grinko et al. [26] analyze yet another entirely Grover-based QAE algorithm and show an empirical improvement over previous counterparts. While all of these algorithms remove the requirement on the QFT that the canonical QAE uses, they all require measurements to estimate the target probability α . However, we utilize QAE as an intermediate step for estimating the mean of our QLGA distribution, which we follow with a minimum-finding routine. Therefore, we require the QAE algorithm to be coherent, and for this reason rely on the canonical QAE instead of the more modern counterparts.

3 Parallel OLGA Time Evolution and Quantity Accumulation

This section describes the parallel QLGA time evolution algorithm and its building blocks. We first detail the quantum register setup and analyze the complexity of known building blocks in the linear qubit encoding. We follow with a description of parallel time evolution and efficient quantity accumulation and conclude the section with a discussion of alternative encoding methods.

3.1 Quantum Register Setup and Base Operations

Throughout this section, we assume that we are addressing distinct lattice configurations that have N_g gridpoints and q velocity channels each, following the commonplace $\mathrm{D}_d\mathrm{Q}_q$ notation. We further assume that we are optimizing over a finite set \mathcal{L} , with $\|\mathcal{L}\|$ lattice distinct configurations. The number of qubits required to implement the linear encoding for a single lattice is simply qN_q , which we refer to as the base register B.

Within the base register, a single layer of $\mathcal{O}(N_g)$ single-qubit gates is required to implement uniformly distributed initial conditions. The $\mathcal{O}(1)$ depth of this operation is one of the computational advantages of the linear encoding over its logarithmically compressed counterparts. The streaming step can be implemented by means of q parallel applications of N_g-1 swap gates per streaming direction, each of depth $\lceil \log_2 N_g \rceil$ [53, 22]. Another advantage of the the linear encoding is that the complexities related to efficiently applying typical bounce-back and specular reflection boundary conditions around solid geometries are largely eliminated. Since the boundary conditions remain consistent across all instances of the superposed LGA states of a single configuration, and since the grid information is not compressed, there is no need to control boundary condition applications on any ancillary state. As a result, the imposition of boundary conditions discussed in [52] and [22] on geometries with a perimeter spanning N_{bc} gridpoints requires $\mathcal{O}(qN_{bc})$ swap gates that act completely in parallel, with depth 1. The cost and application of boundary conditions is consistent with the description of [22].

In addition to the base register, we require 5 additional registers for our algorithm. First is a marker register M that we use to distinguish between the $\|\mathcal{L}\|$ lattice configurations. We shall henceforth assume a maximally compressed representation of this data by encoding the markers into $\lceil \log_2 \|\mathcal{L}\| \rceil$ qubits, and assigning each basis state to a configuration. We discuss an alternative encoding and its tradeoffs in Section 3.4. Second is a data accumulation register D in which the algorithm tracks the total value of the QoI throughout the algorithm. For a problem in which we are interested in tracking a scalar quantity over a region Ω for $N_{t,acc}$ time steps, we generally require at most $\lceil \log_2 (N_{t,acc} \cdot \|\Omega\| \cdot (q+1)) \rceil$ qubits. We provide more details about this choice in Section 3.3. Third, we require an additional, single-qubit "coin" register C, which we use to transform our state into a form that is suitable for the application of QAE and unstructured search. A fourth register E of size e is assigned for running the amplitude estimation routine, and its size e register is left as a choice to the user. Finally, we use 1 more qubit G to distinguish good states during Grover search. The total number of qubits our algorithm uses is therefore

$$N_{q} = \underbrace{qN_{g}}_{\text{Base qubits}} + \underbrace{\lceil \log_{2} \|\mathcal{L}\| \rceil}_{N_{q,acc} \cdot \text{Accumulation qubits}} + \underbrace{\lfloor \log_{2} \left(N_{t,acc} \cdot \|\Omega\| \cdot (q+1)\right) \rceil}_{N_{q,acc} \cdot \text{Accumulation qubits}} + \underbrace{QAE \text{ qubits}}_{Coin \text{ and Grover qubits}}$$

$$(9)$$

For the application to QLBM algorithms, the base register qubit count is typically reduced to $\lceil \log_2 q \rceil + \lceil \log_2 N_g \rceil$ by virtue of the amplitude-based encoding. The accumulation register may be omitted in both cases, should the method be applied to a single time step.

3.2 Parallel QLGA Time Evolution of Configurations

The parallel-configuration QLGA algorithm closely resembles the core QLGA loop, with two key exceptions. The base operations of streaming and collision are used identically as in the QLGA algorithm and retain the same semantics throughout. Where the parallel QLGA algorithm differs is in its application of initial and boundary conditions. Unlike streaming and collisions, these operations cannot be applied uniformly across configurations, since the their semantics are the only differentiation between lattice configurations. It is for this purpose that we employ the marker register M to distinguish between lattice. A straightforward way to implement the different configuration-specific semantics is to control the application of initial and boundary conditions on the state of the marker.

To realize this implementation, we set the state of the register to the uniform superposition $|u\rangle_{\rm M}=1/\sqrt{\|\mathcal{L}\|}\sum_{j=0}^{\|\mathcal{L}\|-1}|j\rangle$, and assign each basis state $|j\rangle$ to represent a lattice. Using this information, we can simply iterate through each basis state to control the configuration-specific semantics. Since both (uncontrolled) uniform initial conditions and reflection

boundary conditions can be applied in parallel with a depth of 1, and there are $\lceil \log_2 \|\mathcal{L}\| \rceil$ control qubits, one can implement the controlled counterparts of the operations of a lattice L using $N_{bc,L}$ $C^{\lceil \log_2 \|\mathcal{L}\| \rceil} X$ gates.

Applying sequential boundary condition imposition for all geometry across all configurations and using the gate decomposition introduced by Barenco et al. [2] leads to a circuit with size and depth of $\mathcal{O}(N_{bc,L_{\max}} \cdot \|\mathcal{L}\| \cdot \log^2 \|\mathcal{L}\|)$, where L_{\max} denotes the lattice with the geometry that spans the largest number of gridpoints. The first two terms stem from the serialized imposition across all gridpoints of all lattices, while the quadratic logarithmic term is due to the CX decomposition. Importantly, the streaming and collision circuits used in QLGA are entirely agnostic of the marker register. This, in turn, means the complexity of these steps remains unaffected by the additions of our algorithm.

Exploiting overlap. One can reduce the cost of enforcing configuration-specific semantics if several configurations share common features. For a particular feature of the configuration of L, let \mathcal{V}_L denote the finite set of velocity channels involved in enforcing the semantics of the feature. For two different configurations, L_j and L_k , the intersection $\mathcal{V}_{L_j} \cap \mathcal{V}_{L_k} \neq \emptyset$ provides an opportunity to enforce the conditions of both configurations using fewer control qubits. One can do this in two steps: first permuting the basis states $|j\rangle$ and $|k\rangle$ into the $|1\rangle^{\otimes \lceil \log_2 \|\mathcal{L}\| \rceil - 1} |0\rangle$ and $|1\rangle^{\otimes \lceil \log_2 \|\mathcal{L}\| \rceil - 1} |1\rangle$ states, and second controlling the operation only on the first $\lceil \log_2 \|\mathcal{L}\| \rceil - 1$ qubits. In general, for an overlapping region of k lattices such that $\bigcap_{j=1}^k \mathcal{V}_{L_{j-1}} \neq \emptyset$, one can reduce the number of controls of the semantics of $\lceil \log_2 k \rfloor$ of these lattices to $\lceil \log_2 \|\mathcal{L}\| \rceil - \lfloor \log_2 k \rfloor$. Asymptotically, this method is in fact worse than the non-overlapping counterpart, since permutations generally require quadratically many one-and two qubit gates to implement [31]. Clearly, addressing all exponentially many possible intersections is extremely inefficient. However, intelligently exploiting scenarios in which the intersections of different lattices are sizeable (i.e., assessing how small differences in airfoil design affect drag at the leading edge of an airplane) and appear in many configurations can lead to significant practical improvements.

We note that in instances where the number of lattices we simulate is not a power of 2, some marker qubit states remain unused. Following the initialization of the system, the quantum state would therefore contain some basis states $|0\rangle_{\rm B}^{\otimes qN_g}|k\rangle_{\rm M}$ for the basis states k that are unassigned. Following the common QLGA semantics, neither collision nor streaming can alter such states as they would otherwise violate mass and momentum conservation. We therefore do not include such cases in the rest of the analyses in this paper.

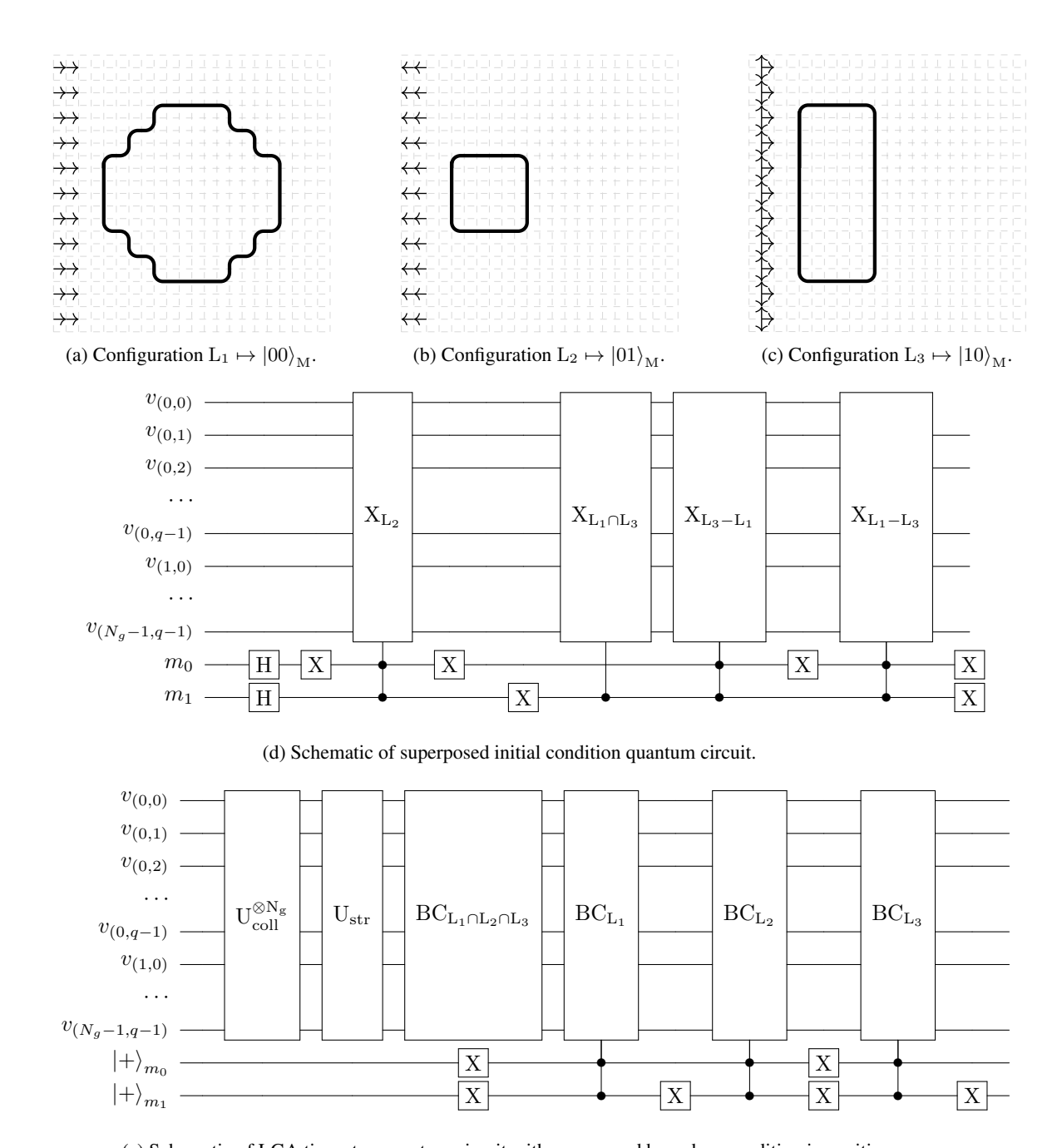
Example. To help provide a more intuitive understanding of how superposed semantics can be implemented in practice, we provide an example of 3 distinct lattices, as depicted in Figure 3a, Figure 3b, and Figure 3c, first in terms of initial conditions and then in terms of boundary treatment. In all 3 lattices, the arrows indicate the initial state of the flow field, while the black outlines delimitate the perimeters of three different boundary-conditioned objects. Our algorithm for this instance requires qN_g qubits for the QLGA loop, and only two additional qubits to mark the three lattice configurations.

The initial state of the system is therefore $|0\rangle_B^{\otimes qN_g}|++\rangle_M$. To impose the initial conditions effectively, we first notice that while the initial state of L_2 does not overlap with the two other lattices, there is a significant overlap between L_1 and L_3 . Using this information, we can devise a quantum circuit that implements these semantics with sequential steps that address L_2 controlled on both marker qubits, the shared semantics $\mathcal{V}_{L_1} \cap \mathcal{V}_{L_3}$ controlled on only one of the marker qubits, and the remainder $\mathcal{V}_{L_1} - \mathcal{V}_{L_3}$ and $\mathcal{V}_{L_3} - \mathcal{V}_{L_1}$, respectively. The schematic implementing this routine is depicted in Figure 3d.

Once the initial conditions are set, the usual QLGA streaming and collision steps can commence completely agnostically of the marker qubits, as depicted by the first 2 operations of Figure 3e. Next, analyzing the properties of the boundary conditions of the three systems we observe that there is a shared segment between the three objects, namely the left wall of the square of L_2 . We can enforce the boundary conditions of this wall using the standard $\mathcal{O}(1)$ depth circuit afforded by the linear encoding completely in parallel from the rest of the boundary conditions. Following this step, we can proceed by iterating through the remainder geometries sequentially, accounting for the shared segments that should not be repeated. This circuit can then be repeated for all time steps without modification.

3.3 Quantity Accumulation

Though the QLGA and QLBM literature has introduced several techniques for computation of physical quantities out of the quantum state without the use of quantum state tomography [54, 19, 23], these techniques have all focused on extracting the information out of the quantum state at a given time step by means of measurement. In contrast, we require a circuit that coherently *accumulates* the required quantity across multiple time steps. Before describing the design of our circuit, we first analyze the properties of the quantities that one might want to query in the QLGA algorithm.



(e) Schematic of LGA time step quantum circuit with superposed boundary condition imposition.

Figure 3: Example of the parallel QLGA circuit for a set of 3 lattices with intersecting initial and boundary conditions.

Within the LGA discretization, physical quantities such as mass, momentum, and forces can all be computed based on the boolean particle occupancies [68]. This in turn means that even more complex quantities, such as drag and lift coefficients, can be computed linearly and coherently from the quantum state. Moreover, the boolean weights of particles make it such that physical quantities can be expressed proportionally to the Hamming weight of the bitstrings encoding the gridpoints within the region of interest. The only exception to this rule is that it is common for discretizations to include a so-called *rest particle*, which is typically assigned twice the mass of regular particles. Accounting for this, we require a circuit that computes the function

$$f(\Omega) \propto \sum_{x \in \Omega} \sum_{j \in \mathcal{V}} \alpha_j x_j \tag{10}$$

with Ω the region of interest, x the gridpoints within this section, \mathcal{V} the set of velocity channels that contribute to the QoI we compute, and α_j the mass of the velocity channel in lattice units. For commonplace discretizations, $\alpha_j \in \{1,2\}$. We can easily derive an upper bound for the number of qubits required to store this value throughout our computation by leveraging the fact that the value of this sum is at most $\|\mathcal{V}\| + 1$ (accounting for the rest particle) for each gridpoint and each time step, which implies that we require at most

$$N_{q,acc} = \lceil \log_2 \left(N_{t,acc} \cdot ||\Omega|| \cdot (q+1) \right) \rceil \tag{11}$$

qubits to retain this value without overflow. To efficiently accumulate this quantity, we introduce a Modified Hamming Weight Adder (MHWA) based on the design of the Draper Adder [13].

The Draper Adder was originally designed to perform addition between two registers, such that the such that $U|x\rangle|y\rangle = |x\rangle|x+y\rangle$, by means of the Quantum Fourier Transform (QFT) and (controlled) phase gates [13]. Our modified adder instead performs the operation

$$U_{\text{MHWA}} |x\rangle |y\rangle = |x\rangle \left| y + \sum_{j=0}^{\|x\|-1} \alpha_j x_j \right\rangle.$$
 (12)

To implement this operation, we can fix the parameters of the controlled phase gates that are applied to the Fourier-transformed $|y\rangle$ state such that the operation effectively implements $U_P|y\rangle = |y+1\rangle$ controlled on the state of a single qubit of $|x\rangle$. This is the same technique as used in the controlled streaming operator described by Schalkers and Möller [52], and the parameters of the phase gates can be easily adjusted to accommodate the weight of the rest particle at no additional complexity cost. We can then iterate through all qubits of $|x\rangle$ repeating this operation to obtain the exact form described in Equation (12).

The integration of this procedure within the parallel-configuration QLGA loop is straightforward, and can be implemented as depicted in Figure 4. We begin by initializing the data register D to the QFT of the vacuum state and perform the QLGA loop in parallel. To accumulate the quantities, we perform iterative controlled phase gates at the end of each time step, where the controls are the qubits that correspond to the region of interest Ω . Note that unless the QLGA loop has reached its end, there is no need to perform the inverse QFT, as following accumulation steps require the data qubits to be in Fourier space. As such, for each time step, we execute only the controlled phase gates (depicted succinctly as the P gates in Figure 4) and map the qubits back to the computational basis at the end of the computation. Furthermore, this implementation is entirely independent of the marker register, as we are comparing the same QoI across all configurations. Assuming $N_{q,acc}$ is the number of accumulation qubits as described by Equation (9), the MHWA circuit can be realized using exactly $\|\Omega\|N_{q,acc}$ controlled phase gates, in addition to the $\mathcal{O}\left(N_{q,acc}^2\right)$ gates required to implement the QFT blocks. The depth of the controlled phase array can be reduced to $\mathcal{O}\left(\|\Omega\|+N_{q,acc}\right)$, as each qubit of the accumulation register is addressed independently. Following the application of N_t time steps consisting of interleaving QLGA and accumulation steps, we obtain a quantum state of the form

$$|\psi_{\text{LGA}}\rangle = \sum_{j} |\psi_{L_{j}}\rangle_{\text{B}} |f(L_{j}, \Omega)\rangle_{\text{D}} |j\rangle_{\text{M}} |0\rangle_{\text{C}} |0\rangle_{\text{E}}^{\otimes e} |0\rangle_{\text{G}}.$$
(13)

3.4 Alternative Encodings

Before considering the optimization part of our algorithm, we briefly consider the effects that different encoding choices entail. We first analyze the consequences of encoding choices of the marker register, before assessing the application of our methods to algorithms that utilize different encodings in the base register.

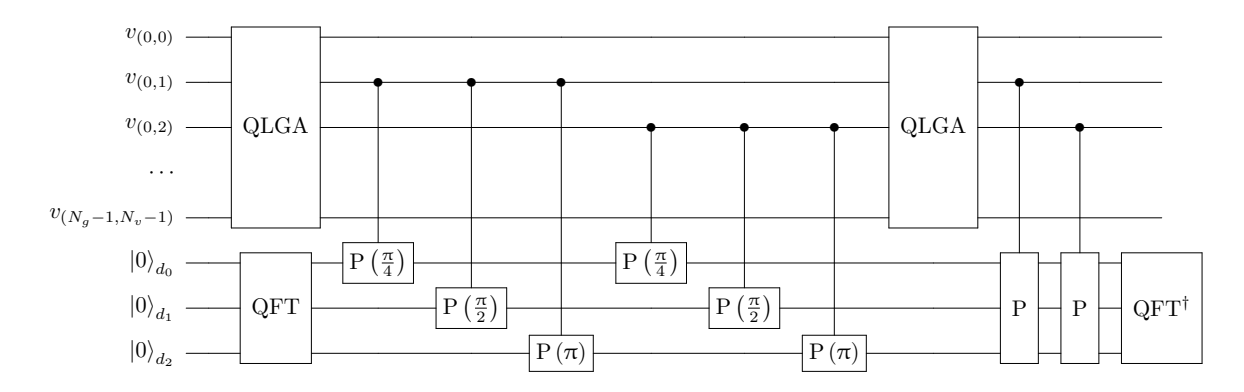


Figure 4: Schematic of Modified Hamming Weight Adder quantum circuit.

Marker register encodings. Thus far, we assumed a maximally compressed encoding of the marker register due to its qubit efficiency. However, this method requires heavily controlled applications in instances in which configurations share little overlap. An alternative marker register data structure that alleviates this limitation is the *one-hot encoding*. In the one-hot encoding, we use $\|\mathcal{L}\|$ marker qubits, and assign each configuration a state

$$|\mathbf{e}_{j}\rangle = |0\rangle^{\otimes j} |1\rangle |0\rangle^{\otimes \|\mathcal{L}\| - j - 1},$$
 (14)

for $0 \le j \le \|\mathcal{L}\| - 1$. This encoding makes it such that each configuration can be identified by a single qubit, instead of by entire marker register. While the qubit requirement increases from $\mathcal{O}(\log_2 \|\mathcal{L}\|)$ in the maximally compressed scenario to $\mathcal{O}(\|\mathcal{L}\|)$ for the one-hot alternative, the semantics of the linear encoding QLGA boundary conditions allow for a significant gate count and depth reduction. Since boundary conditions of disjoint geometries can be enforced fully in parallel, and since each configuration is identified by a single qubit, we can therefore apply disjoint boundary condition circuits on arbitrarily many lattices by adding a single control to the appropriate swap gates. While the number of gates still scales with the perimeter of the geometry, the depth of this circuit is $\mathcal{O}(1)$ due to disjoint controls and targets.

Which of the two register encoding strategies is superior in practice is highly dependent on the application and the resources available. For highly disjointed geometries and hardware with large numbers of qubits, the one-hot encoding preserves the parallel application of boundary conditions, which is a significant advantage of the linear QLGA encoding. For hardware that is limited in the number of qubits, but where the computational budget is more permissive and where overlap can be strategically exploited, the maximally compressed encoding might become preferable, if the additional cost associated with the decomposition of multi-controlled X gates is admissible.

Base register encodings. Thus far we have analyzed our algorithm in the linear encoding of the base register due to its expressivity and computational advantages. However, many QLGA and QLBM algorithms explore the amplitude-based encoding, thanks to its logarithmic memory compression of the grid register [9, 10, 52, 56, 64]. While our marker encoding and boundary conditions schemes can be readily applied with consistent qubit requirements and computational complexity analyses, QoI handling requires more consideration. In amplitude-based encodings, the quantity accumulation method described previously does not apply, as the physical components that contribute to the QoIs are tied to amplitudes, rather than Hamming weights. Previous work by Schalkers and Möller [54] and Georgescu et al. [22] has, however, introduced quantum circuits that accumulate the amplitude spread over physical regions of space onto a single ancillary qubit, with particularly efficient implementations for regions that can be bounded by axis-aligned and diagonal boundaries. While these methods differ from our implementation, and can only be directly utilized for one time step, they nonetheless construct a quantum state that is exactly of the form we need, as we explore in Section 4.1.

Though computationally expensive, addressing the multiple time step scenario is also possible by applying multiple controlled state evolution operators as is the case in, for instance, quantum phase estimation. We note that accumulating the quantity over multiple time steps is not a necessity for all practical applications. Instances in which QoIs are computed once the flow has reached a steady state lend themselves particularly well to the single-time step case.

4 Mean Estimation and Minimum Finding

This section describes how established quantum algorithms can be used to query the ensemble average LGA quantum state given in Equation (13) to find the optimal lattice configuration. Section 4.1 describes how we can efficiently transform the quantum state into a form that is suitable for the usage of the Dürr-Høyer algorithm, which is covered in Section 4.2. For applications to the QLBM, the amplitude accumulation method described by Schalkers and Möller [54] can be applied to obtain the appropriate quantum state without the techniques described in this section.

4.1 Amplitude Mapping and Mean Estimation

The problem of estimating the mean of a (Monte Carlo) quantum algorithm \mathcal{A} has been studied extensively in the literature. Heinrich [30] and Brassard et al. [8] introduced two such asymptotically optimal algorithms that obtain the typical quadratic speedup associated with "Grover-like" routines. Montanaro [47] later described how these methods can yield this quadratic advantage in tandem with quantum walks and derived rigorous error bounds by making use the QAE routine. To make use of these methods, we need to transform the state obtained after the application of the QLGA algorithm from Equation (13) into a form that supports the use of QAE. Previous work covers the construction of such oracles for different classes of problems including encoding the mean reward in reinforcement learning [14], computing the centroid distance in clustering problems [67, 38], selecting the best arm of a multi-arm bandit in bandit optimization [63], and topology optimization via finite element solvers in structural mechanics [32]. Such oracles can often be expressed in the form given in Equation (8). Adapting this general form to our LGA setting, we formulate a unitary that acts on the data and coin registers as

$$U_{\rm M} |f(L_j, \Omega)\rangle_{\rm D} |0\rangle_{\rm C} = |f(L_j, \Omega)\rangle_{\rm D} \left(\sqrt{\phi(f)} |1\rangle_{\rm C} + \sqrt{1 - \phi(f)} |0\rangle_{\rm C}\right), \tag{15}$$

while leaving all other registers unaffected. The purpose of this operation is to map the superposed values of the D register onto the coin qubit C such that QAE can then estimate this amplitude. 2 We denote this mapping as a function ϕ , properties of which warrant some careful consideration. Specifically, we require that ϕ is monotone on the support imposed by the data register, such that the minimum finding step can be applied on the QAE of ϕ is consistent with f. Second, we require that the implementation of $U_{\rm M}$ is efficient in the size of the data register. Finally, we require that ϕ imposes an amplitude that is proportional to the ensemble average value of D onto the $|1\rangle$ state of the coin qubit, such that the resulting state matches the goal formulated in Equation (2). In the remainder of this section, we provide two methods implementing such a unitary operation: a weighted rotation method and a linear comparison method.

Weighted Rotation Mapping. The weighted rotation map is implemented by means for a series of single-controlled $R_Y(\theta)$ gates, where the parameter θ is chosen as the weight of the contributing bit, from least to most significant. This operation uses the fact that $R_Y(\theta_0)R_Y(\theta_1) = R_Y(\theta_0 + \theta_1)$ maps the binary representation of a number x as

$$\prod_{j=0}^{N_{q,acc}-1} R_{Y}(\alpha x_{j} 2^{j}) = R_{Y} \left(\sum_{j=0}^{N_{q,acc}-1} \alpha x_{j} 2^{j} \right)$$

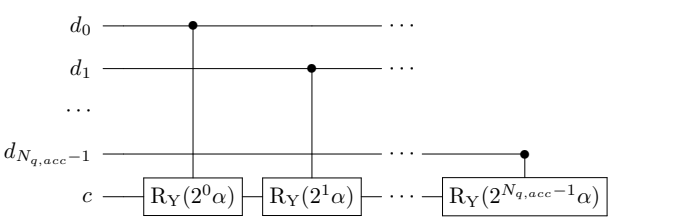
$$= R_{Y} (\alpha x), \tag{16}$$

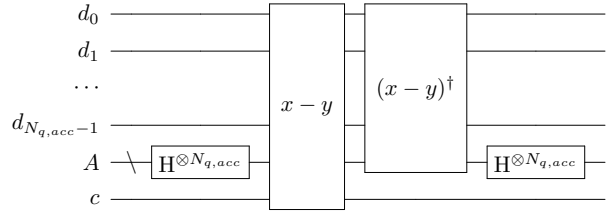
where x_j denotes the state of the j^{th} qubit of x. Acting on the $|0\rangle$ state, this operation sets the amplitude of the $|1\rangle$ state to $\sin(\alpha f(L,\Omega)/2)$. We can enforce the monotonicity of this mapping by setting the value of the free parameter α to restrict the domain ϕ . We know that, by design, $0 \le f(L,\Omega) \le N_{t,acc} \|\Omega\| (q+1) = F_{\max}$, and we can leverage this fact by setting

$$\alpha = \frac{\pi}{F_{\text{max}}} \implies 0 \le \alpha \frac{f(L,\Omega)}{2} \le \frac{\pi F_{\text{max}}}{2F_{\text{max}}} = \frac{\pi}{2}.$$
 (17)

The relation in Equation (17) limits the support of the sinusoidal ϕ function to $[0, \pi/2]$, which is an interval in which both the amplitude \sin and its implied probability \sin^2 are monotonically increasing. This circuit requires precisely $N_{g,acc}$ single-controlled R_Y gates, implemented in series as shown in Figure 5a.

²We note that the usage of amplitude mapping is only required for computational basis state encodings – amplitude-based encodings used widely in QLBM algorithms may use the techniques outlined in [54] and [22] as an efficient alternative.





- (a) Weighted rotation mapping quantum circuit.
- (b) Linear comparison mapping quantum circuit.

Figure 5: Amplitude mapping quantum circuits.

Exact Linear Mapping. A consequence of the sinusoidal shape of the weighted rotation mapping is that not all regions of the landscape are equally distinguishable. This nonlinearity may be beneficial if configurations have values that are in different regions of the landscape, however, it is symmetrically a disadvantage when values are in an area of the sin function with a shallow slope. In such instances, a more consistent mapping may become preferable.

The exact linear mapping can be implemented as follows. In an ancillary register AM, of the same number of qubits as the data accumulation register, we instantiate the uniform superposition $|u\rangle_{\rm AM} = \sum_j 1/\sqrt{N_{q,acc}}\,|j\rangle$. Next, we use a quantum comparison operation, such as the one described by Gidney [24], to compare the values encoded in the data register to $|u\rangle$. This operation flips the state of the coin qubit for all states j less than the value of the data register. This is equivalent to $\phi(f) = \sum_x f_x(\cdot)/2^{N_{q,acc}}$. This form satisfies the monotonicity requirement, and gives an exact linear comparison between different data register values, per marker. A practical advantage of this method is that comparator operations are extensively used in QLGA [22] and QLBM [52] algorithms for the efficient imposition of boundary conditions, and implementations are readily available. The complexity of this step is dominated by the comparison operation, which is quadratic in the size of the data accumulation register. Following the comparison and mapping onto the coin qubit, the state of the ancilla qubits can be reset by undoing the comparison.

Following the application of either amplitude mapping method, our algorithm proceeds by executing the QAE routine to extract the amplitudes of the coin register into the estimation register. Importantly, neither the mapping, nor the QAE steps need to be controlled on the marker. Since the parallel QLGA/QLBM algorithm contains blocks that are controlled on the marker, the application of the Grover iterate $\mathcal{A}_{\text{QLGA}}S_0\mathcal{A}_{\text{QLGA}}^{\dagger}S_T$ is itself block-diagonal in the marker states, which implies that the QAE block acts in parallel for all lattice configurations. While the complexity of the QAE block itself does depend on the cost of $\mathcal{A}_{\text{QLGA}}$, the number of queries is consistent with the typical complexity of $\mathcal{O}(\epsilon^{-1})$ and no further terms are incurred.

The quantum state obtained after application the amplitude mapping and the QAE steps is given by

$$|\psi_{\text{QAE}}\rangle = \sum_{j} |\psi_{L_{j}}\rangle_{\text{B}} |f(L_{j}, \Omega)\rangle_{\text{D}} |j\rangle_{\text{M}} \left(\sqrt{\phi(f_{j})} |1\rangle_{\text{C}} + \sqrt{1 - \phi(f_{j})} |0\rangle_{\text{C}}\right) |\hat{\phi}_{j}\rangle_{\text{E}} |0\rangle_{\text{G}},$$
(18)

with $\hat{\phi}$ the estimated parameter such that $\sin^2\left(\pi\hat{\phi}_j/2^e\right)\approx\phi(f(L_j,\Omega))$. The final step of our method uses iterative Grover search over the estimation register to find the lattice configuration with the minimum estimated mean QoI.

4.2 Minimum Finding and Analysis

The algorithmic steps described thus far can be regarded as part of the state preparation procedure that assembles the state

$$|\psi_{\text{PRE}}\rangle = \frac{1}{\sqrt{\|\mathcal{L}\|}} \sum_{j=0}^{\mathcal{L}} |j\rangle_{\text{M}} \left|\hat{\phi}_{j}\right\rangle_{\text{E}} |0\rangle_{\text{G}},$$
 (19)

with all other registers acting as ancilla space for the computation of the mean QoIs of each lattice configuration. The final step of our algorithm consists of running a minimum finding routine over the register E to find the minimum estimated value and the marker associated with it. For this purpose, we use the Dürr-Høyer algorithm [15], which

combines Grover iterations with exponential search. Intuitively, the Dürr-Høyer routine consists of tracking a threshold τ that is used to partition $|\psi_{PRE}\rangle$ into "good" states that fall below the threshold and "bad" states that exceed τ as

$$|\psi_{\rm DH}\rangle = \frac{1}{\sqrt{\|\mathcal{L}\|}} \sum_{j=0}^{\|\mathcal{L}\|-1} |j\rangle_{\rm M} \left| \hat{\phi}_j \right\rangle_{\rm E} \left| \hat{\phi_j} < \tau \right\rangle_{\rm G}, \tag{20}$$

which follows exactly the typical Grover partition form given in Equation (8). This operation only requires one additional comparator operation between the estimated value and the threshold τ , which can be reversibly implemented without the use of any ancillary register [52]. Within the Grover search framework, the QLGA \rightarrow amplitude mapping \rightarrow QAE \rightarrow threshold comparison, followed by the application of a single Z gate on the G qubit, can be regarded as the implementation of a phase query gate as described in Section 2.3.1. By amplifying the amplitudes of the "good" states that fall below the threshold, the Dürr-Høyer routine can then measure the outcome of the E register and update the threshold if a lower value is measured. By selecting appropriate update parameters, the typical quadratic Grover search advantage is preserved, up to a multiplicative constant [15]. Tying together the query complexity of the minimum finding loop and the one- and two-qubit gate cost of the parallel QLGA primitives, we obtain a computational complexity of

$$\mathcal{O}\left(\underbrace{\sqrt{\|\mathcal{L}\|}}_{\text{Dürr-Høyer}} \cdot \underbrace{\frac{\text{QAE}}{\epsilon}}_{\epsilon} \cdot N_{t} \cdot \left(\underbrace{2^{q} + \log_{2} N_{g}}_{\text{QLGA}} + \underbrace{\log_{2}^{2} \left(N_{t,acc} \cdot \|\Omega\| \cdot (q+1)\right)}_{\text{QLGA}} + \underbrace{N_{bc,L_{\max}} \cdot \|\mathcal{L}\| \cdot \log^{2} \|\mathcal{L}\|}_{\text{Parallel Semantics}}\right)\right). \tag{21}$$

Equation (21) gives a quadratic improvement in the size of the lattice configuration and in the additive error estimate. The estimate assumes that initial conditions can be implemented with a cost that is of the same order as boundary condition imposition, and accumulation terms absorbs the cost of the amplitude mapping step. The cost of the Dürr-Høyer comparison and that of the amplitude mapping step are both absorbed by the accumulation term, which is preformed for multiple time steps. The QLBM analog would alter the cost of collision and parallel semantics depending on the implementation. While the cost of the collision operator varies significantly depending on the target equation and approximation, the parallel boundary condition imposition can inherit the polylogarithmic scaling in the grid size as described in [52] and [22]. This analysis does not account for the advantage gained by exploiting configuration overlap, as it is a highly application-dependent.

Error reduction techniques. To ensure that the Dürr-Høyer algorithm bounds and precision are consistent with the theoretical formulation, we must ensure that the errors incurred by the previous steps are appropriately bounded. In particular we are concerned with whether the the QAE approximation error ϵ affects the outcome of the minimum finding routine. For an amplitude ϕ and a positive number of iterations l, the canonical QAE is known to output an estimate $\hat{\phi}$ that satisfies

$$|\phi - \hat{\phi}| \le 2\pi \frac{\sqrt{\phi(1-\phi)}}{l} + \left(\frac{\pi}{l}\right)^2 \tag{22}$$

with probability at least $8/\pi^2$ [7, 67]. Furthermore, we consider the gap

$$\Delta = \min_{L \neq L^*} \left[\phi(f(L, \Omega)) - \phi(f(L^*, \Omega)) \right]$$
(23)

between the true optimal solution and the closest other configuration. In our strictly monotone construction of ϕ , errors can occur in instances when QAE precision leads to misclassifications in the oracle $[\hat{\phi} < \tau]$ as a result of Δ falling in this range. This is an instance of a *bounded-error oracle* [33], which can be mitigated in several ways. Høyer et al. [33] show that interleaving amplitude amplification invocations with an error-reduction steps retains the asymptotic scaling of quantum search in instances where the oracle error is bounded. The error reduction routine consists of stochastically checking whether solutions marked by the oracle are, in fact, true positives, and performing majority voting on the outcome to "push back" false positives [33]. Wiebe et al. [67] also approach the error reduction problem with a majority voting based scheme, which uses superposed copies of the QAE estimate to compute the median of the parallel QAE runs. Both of these techniques can be applied to our algorithm in a straightforward manner.

5 Conclusion

This work highlighted the connection between Quantum CFD algorithms and Optimization techniques in a way that circumvents the requirement of flow field measurement altogether. We detailed how simple modifications to initial condition calculations and boundary condition imposition enable the simulation of many lattice configurations in parallel. We showed how shared properties of candidate configurations can be leveraged to increase the efficiency of the parallel QLGA algorithm. Finally, we described two techniques to transform the quantum state into a form that enables algorithms from discrete optimization and machine learning to apply directly to our problem. Throughout the paper, we provided gate-level descriptions and computational complexity analyses of the circuits we developed. With small modifications, the methods described in this paper apply to both QLGA and QLBM algorithms.

Research at the intersection of Quantum CFD and Optimization could follow several directions, three of which we address here. First, the development of specialized Grover diffusion operators for QLGA and QLBM routines that are more efficient than inverting the algorithm at the gate level could provide significant practical performance improvements. Second, developing methods for QLBM algorithms that make use of measurement and dynamic circuits (and therefore violate the coherence assumptions we rely on in our analysis) would improve the applicability of the discussed methods. Finally, an error analysis that links physical properties of the system, such as the Reynolds number, to the accuracy and reliability of the estimation and minimum finding blocks would provide deeper insight into the class of problems that Quantum CFD could help solve in the future.

6 Acknowledgements

We gratefully acknowledge support from the joint research program *Quantum Computational Fluid Dynamics* by Fujitsu Limited and Delft University of Technology, co-funded by the Netherlands Enterprise Agency under project number PPS23-3-03596728.

References

- [1] Scott Aaronson and Patrick Rall. Quantum approximate counting, simplified. In *Symposium on simplicity in algorithms*, pages 24–32. SIAM, 2020.
- [2] Adriano Barenco, Charles H Bennett, Richard Cleve, David P DiVincenzo, Norman Margolus, Peter Shor, Tycho Sleator, John A Smolin, and Harald Weinfurter. Elementary gates for quantum computation. *Physical review A*, 52(5):3457, 1995.
- [3] Prabhu Lal Bhatnagar, Eugene P Gross, and Max Krook. A model for collision processes in gases. i. small amplitude processes in charged and neutral one-component systems. *Physical review*, 94(3):511, 1954.
- [4] Bruce M Boghosian and Washington Taylor. Quantum lattice-gas models for the many-body schrödinger equation. *International Journal of Modern Physics C*, 8(04):705–716, 1997.
- [5] Bruce M Boghosian and Washington Taylor IV. Simulating quantum mechanics on a quantum computer. *Physica D: Nonlinear Phenomena*, 120(1-2):30–42, 1998.
- [6] Michel Boyer, Gilles Brassard, Peter Høyer, and Alain Tapp. Tight bounds on quantum searching. *Fortschritte der Physik: Progress of Physics*, 46(4-5):493–505, 1998.
- [7] Gilles Brassard, Peter Hoyer, Michele Mosca, and Alain Tapp. Quantum amplitude amplification and estimation. *arXiv preprint quant-ph/0005055*, 2000.
- [8] Gilles Brassard, Frederic Dupuis, Sebastien Gambs, and Alain Tapp. An optimal quantum algorithm to approximate the mean and its application for approximating the median of a set of points over an arbitrary distance. *arXiv* preprint arXiv:1106.4267, 2011.
- [9] Ljubomir Budinski. Quantum algorithm for the advection–diffusion equation simulated with the lattice boltzmann method. *Quantum Information Processing*, 20(2):57, 2021.
- [10] Ljubomir Budinski. Quantum algorithm for the navier–stokes equations by using the streamfunction-vorticity formulation and the lattice boltzmann method. *International Journal of Quantum Information*, 20(02):2150039, 2022.
- [11] Andrew M Childs and Nathan Wiebe. Hamiltonian simulation using linear combinations of unitary operations. *arXiv preprint arXiv:1202.5822*, 2012.
- [12] Reuben Demirdjian, Daniel Gunlycke, Carolyn A Reynolds, James D Doyle, and Sergio Tafur. Variational quantum solutions to the advection–diffusion equation for applications in fluid dynamics. *Quantum Information Processing*, 21(9):322, 2022.

- [13] Thomas G Draper. Addition on a quantum computer. arXiv preprint quant-ph/0008033, 2000.
- [14] Vedran Dunjko, Jacob M Taylor, and Hans J Briegel. Quantum-enhanced machine learning. *Physical review letters*, 117(13):130501, 2016.
- [15] Christoph Durr and Peter Hoyer. A quantum algorithm for finding the minimum. *arXiv preprint quant-ph/9607014*, 1996.
- [16] Esmaeil Esmaeilifar, Doyeol Ahn, and Rho Shin Myong. Quantum algorithm for nonlinear burgers' equation for high-speed compressible flows. *Physics of Fluids*, 36(10), 2024.
- [17] Terry Farrelly. A review of quantum cellular automata. Quantum, 4:368, 2020.
- [18] Niccolò Fonio, Pierre Sagaut, Ljubomir Budinski, and Valtteri Lahtinen. Adaptive lattice-gas algorithm: Classical and quantum implementations. *Physical Review E*, 112(3):035302, 2025.
- [19] Niccolò Fonio, Pierre Sagaut, and Giuseppe Di Molfetta. Quantum collision circuit, quantum invariants and quantum phase estimation procedure for fluid dynamic lattice gas automata. *Computers & Fluids*, 299:106688, 2025. ISSN 0045-7930.
- [20] Uriel Frisch, Brosl Hasslacher, and Yves Pomeau. Lattice-gas automata for the navier-stokes equation. *Physical review letters*, 56(14):1505, 1986.
- [21] Frank Gaitan. Finding flows of a navier–stokes fluid through quantum computing. *npj Quantum Information*, 6(1): 61, 2020.
- [22] Călin A Georgescu, Merel A Schalkers, and Matthias Möller. Fully quantum lattice gas automata building blocks for computational basis state encodings. *arXiv preprint arXiv:2506.12662*, 2025.
- [23] Călin A Georgescu, Merel A Schalkers, and Matthias Möller. qlbm–a quantum lattice boltzmann software framework. *Computer Physics Communications*, page 109699, 2025.
- [24] Craig Gidney. Factoring with n+ 2 clean qubits and n-1 dirty qubits. arXiv preprint arXiv:1706.07884, 2017.
- [25] Peyman Givi, Andrew J Daley, Dimitri Mavriplis, and Mujeeb Malik. Quantum speedup for aeroscience and engineering. *AIAA Journal*, 58(8):3715–3727, 2020.
- [26] Dmitry Grinko, Julien Gacon, Christa Zoufal, and Stefan Woerner. Iterative quantum amplitude estimation. *npj Quantum Information*, 7(1):52, 2021.
- [27] Lov K Grover. A fast quantum mechanical algorithm for database search. In *Proceedings of the twenty-eighth annual ACM symposium on Theory of computing*, pages 212–219, 1996.
- [28] Lov K Grover. Quantum mechanics helps in searching for a needle in a haystack. *Physical review letters*, 79(2): 325, 1997.
- [29] J Hardy, Yves Pomeau, and O De Pazzis. Time evolution of a two-dimensional model system. i. invariant states and time correlation functions. *Journal of Mathematical Physics*, 14(12):1746–1759, 1973.
- [30] Stefan Heinrich. Quantum summation with an application to integration. *Journal of Complexity*, 18(1):1–50, 2002.
- [31] Steven Herbert, Julien Sorci, and Yao Tang. Almost-optimal computational-basis-state transpositions. *Physical Review A*, 110(1):012437, 2024.
- [32] Leonhard Hölscher, Oliver Ahrend, Lukas Karch, Carlotta L'Estocq, Marc Marfany Andreu, Tobias Stollenwerk, Frank K Wilhelm, and Julia Kowalski. End-to-end quantum algorithm for topology optimization in structural mechanics. *arXiv preprint arXiv:2510.07280*, 2025.
- [33] Peter Høyer, Michele Mosca, and Ronald De Wolf. Quantum search on bounded-error inputs. In *International Colloquium on Automata, Languages, and Programming*, pages 291–299. Springer, 2003.
- [34] Wael Itani. Towards a Quantum Algorithm for Lattice Boltzmann (QALB) Simulation With a Nonlinear Collision Term. New York University Tandon School of Engineering, 2025.
- [35] Wael Itani and Sauro Succi. Analysis of carleman linearization of lattice boltzmann. Fluids, 7(1):24, 2022.
- [36] Wael Itani, Katepalli R. Sreenivasan, and Sauro Succi. Quantum algorithm for lattice boltzmann (qalb) simulation of incompressible fluids with a nonlinear collision term, 2023. URL https://arxiv.org/abs/2304.05915.
- [37] Christopher L Jawetz, Zhixin Song, Spencer H Bryngelson, and Alexander Alexeev. Quantum lattice boltzmann algorithm for heat transfer with phase change. *arXiv preprint arXiv:2509.21630*, 2025.
- [38] Iordanis Kerenidis, Jonas Landman, Alessandro Luongo, and Anupam Prakash. q-means: A quantum algorithm for unsupervised machine learning. *Advances in neural information processing systems*, 32, 2019.

- [39] Sriharsha Kocherla, Zhixin Song, Fatima Ezahra Chrit, Bryan Gard, Eugene F Dumitrescu, Alexander Alexeev, and Spencer H Bryngelson. Fully quantum algorithm for mesoscale fluid simulations with application to partial differential equations. *AVS Quantum Science*, 6(3), 2024.
- [40] Timm Krüger, Halim Kusumaatmaja, Alexandr Kuzmin, Orest Shardt, Goncalo Silva, and Erlend Magnus Viggen. The lattice boltzmann method. *Springer International Publishing*, 10(978-3):4–15, 2017.
- [41] Oleksandr Kyriienko, Annie E Paine, and Vincent E Elfving. Solving nonlinear differential equations with differentiable quantum circuits. *Physical Review A*, 103(5):052416, 2021.
- [42] Monica Lăcătuş and Matthias Möller. Surrogate quantum circuit design for the lattice boltzmann collision operator. *arXiv preprint arXiv:2507.12256*, 2025.
- [43] Peter Love. On quantum extensions of hydrodynamic lattice gas automata. Condensed Matter, 4(2):48, 2019.
- [44] Mori Mani and Andrew J Dorgan. A perspective on the state of aerospace computational fluid dynamics technology. *Annual Review of Fluid Mechanics*, 55(1):431–457, 2023.
- [45] David A Meyer. From quantum cellular automata to quantum lattice gases. *Journal of Statistical Physics*, 85: 551–574, 1996.
- [46] David A Meyer. Quantum lattice gases and their invariants. *International Journal of Modern Physics C*, 8(04): 717–735, 1997.
- [47] Ashley Montanaro. Quantum speedup of monte carlo methods. *Proceedings of the Royal Society A: Mathematical, Physical and Engineering Sciences*, 471(2181):20150301, 2015.
- [48] Aaron Nagel and Johannes Löwe. Quantum lattice boltzmann method for multiple time steps without reinitialization for linear advection-diffusion problems. *arXiv preprint arXiv:2510.05965*, 2025.
- [49] Ashwin Nayak and Felix Wu. The quantum query complexity of approximating the median and related statistics. In *Proceedings of the thirty-first annual ACM symposium on Theory of computing*, pages 384–393, 1999.
- [50] Claudio Sanavio and Sauro Succi. Lattice boltzmann–carleman quantum algorithm and circuit for fluid flows at moderate reynolds number. AVS Quantum Science, 6(2), 2024.
- [51] Claudio Sanavio, William A. Simon, Alexis Ralli, Peter Love, and Sauro Succi. Carleman-lattice-boltzmann quantum circuit with matrix access oracles, 2025. URL https://arxiv.org/abs/2501.02582.
- [52] Merel A Schalkers and Matthias Möller. Efficient and fail-safe quantum algorithm for the transport equation. *Journal of Computational Physics*, 502:112816, 2024.
- [53] Merel A Schalkers and Matthias Möller. On the importance of data encoding in quantum boltzmann methods. *Quantum Information Processing*, 23(1):20, 2024.
- [54] Merel A Schalkers and Matthias Möller. Momentum exchange method for quantum boltzmann methods. Computers & Fluids, 285:106453, 2024.
- [55] Robert R Schaller. Moore's law: past, present and future. IEEE spectrum, 34(6):52–59, 1997.
- [56] Rene Steijl. Quantum algorithms for nonlinear equations in fluid mechanics. *Quantum computing and communications*, 2020.
- [57] Sauro Succi. The lattice Boltzmann equation: for fluid dynamics and beyond. Oxford university press, 2001.
- [58] Yohichi Suzuki, Shumpei Uno, Rudy Raymond, Tomoki Tanaka, Tamiya Onodera, and Naoki Yamamoto. Amplitude estimation without phase estimation: Y. suzuki et al. *Quantum Information Processing*, 19(2):75, 2020.
- [59] Blaga N Todorova and René Steijl. Quantum algorithm for the collisionless boltzmann equation. *Journal of Computational Physics*, 409:109347, 2020.
- [60] John v Neumann and Arthur W Burks. Theory of self-reproducing automata. University of Illinois Press Urbana, 1966.
- [61] Salvador Elías Venegas-Andraca. Quantum walks: a comprehensive review. *Quantum Information Processing*, 11 (5):1015–1106, 2012.
- [62] Boyuan Wang, Zhaoyuan Meng, Yaomin Zhao, and Yue Yang. Quantum lattice boltzmann method for simulating nonlinear fluid dynamics. *arXiv* preprint arXiv:2502.16568, 2025.
- [63] Daochen Wang, Xuchen You, Tongyang Li, and Andrew M Childs. Quantum exploration algorithms for multiarmed bandits. In *Proceedings of the AAAI Conference on Artificial Intelligence*, volume 35, pages 10102–10110, 2021.

- [64] David Wawrzyniak, Josef Winter, Steffen Schmidt, Thomas Indinger, Christian F Janßen, Uwe Schramm, and Nikolaus A Adams. Linearized quantum lattice-boltzmann method for the advection-diffusion equation using dynamic circuits. *Computer Physics Communications*, page 109856, 2025.
- [65] David Wawrzyniak, Josef Winter, Steffen Schmidt, Thomas Indiniger, Christian F Janßen, Uwe Schramm, and Nikolaus A Adams. Dynamic circuits for the quantum lattice-boltzmann method. *arXiv preprint arXiv:2502.02131*, 2025.
- [66] Chu-Ryang Wie. Simpler quantum counting. arXiv preprint arXiv:1907.08119, 2019.
- [67] Nathan Wiebe, Ashish Kapoor, and Krysta M Svore. Quantum nearest-neighbor algorithms for machine learning. *Quantum information and computation*, 15(3-4):318–358, 2015.
- [68] Dieter A Wolf-Gladrow. Lattice-gas cellular automata and lattice Boltzmann models: an introduction. Springer, 2004.
- [69] Jeffrey Yepez. Lattice-gas quantum computation. *International Journal of Modern Physics C*, 9(08):1587–1596, 1998.
- [70] Jeffrey Yepez. Quantum computation of fluid dynamics. In NASA International Conference on Quantum Computing and Quantum Communications, pages 34–60. Springer, 1998.
- [71] Jeffrey Yepez. Quantum lattice-gas model for computational fluid dynamics. *Physical Review E*, 63(4):046702, 2001.
- [72] Jeffrey Yepez. Quantum lattice-gas model for the burgers equation. *Journal of Statistical Physics*, 107:203–224, 2002.
- [73] Antonio David Bastida Zamora, Ljubomir Budinski, Ossi Niemimäki, and Valtteri Lahtinen. Efficient quantum lattice gas automata. *Computers & Fluids*, 286:106476, 2025.
- [74] Antonio David Bastida Zamora, Ljubomir Budinski, Pierre Sagaut, and Valtteri Lahtinen. Lattice gas automata with floating-point numbers: A connection between molecular dynamics and lattice boltzmann method for quantum computers. *Physical Review E*, 112(1):015305, 2025.